VISUALIZATION OF TRANSPORT ACROSS A HORIZONTAL VENT DUE TO DENSITY AND PRESSURE DIFFERENCES

Y. Jaluria, S.H.-K. Lee, G.P. Mercier and Q. Tan
Mechanical and Aerospace Engineering Department
Rutgers University, New Brunswick, New Jersey

ABSTRACT

A very important flow and transport circumstance that arises in practical problems such as enclosure fires is that of heat and mass transfer across a horizontal vent. Such vents exist in enclosed regions such as rooms and energy storage and ventilation systems. It is important to understand the basic nature of the transport processes that arise because of finite, non-zero, density and pressure differences that usually exist across such vents. The flow is driven by these two mechanisms and very complicated flow patterns arise, depending on the governing variables in the problem. For instance, a dominant pressure effect results in a unidirectional flow, whereas significant buoyancy effects lead to a bidirectional flow exchange. The heat and mass transfer associated with the flow is similarly strongly influenced by the flow regime. There is a strong need for visualization to determine if a unidirectional or a bidirectional flow exists across the vent and to study the basic characteristics of the transport processes involved. This paper presents a study of this heat and mass transfer problem employing water and air as the fluid media for two different experimental systems. Pure and saline water are used in the first case to obtain the unstably stratified circumstance with a pressure difference across the vent. Air at different temperature levels is used in the second case. A laser sheet, with smoke, is used for visualization in air and a shadowgraph for water. Other visualization techniques are also used to obtain qualitative and quantitative results on the flow direction, transport rates and the relevant mechanisms. Since transient effects are important in many cases, video recordings are employed to obtain the frequency of observed oscillations in the transport and for determining the transition from one regime to the other. Visualization is crucial to the understanding of these processes and to the determination of the transport regime under various operating conditions.

INTRODUCTION

Buoyancy induced flows generated by fires in enclosures such as rooms have received considerable attention in the literature (Quintiere, 1977, Jaluria, 1980, Jaluria and Cooper, 1989). However, not much work has been done on the flow through openings or vents such as those between containment areas in nuclear power systems, connecting rooms in buildings and between decks in ships. Vertical vents have been studied in recent years because of their importance in several practical problems, such as room fires and electronic and energy systems (Gebhart et al.,1988 and Abib and Jaluria,1988). In the mathematical modeling of room fires, the flow rate through a vertical opening is often obtained by using Bernoulli's equation along with a flow discharge coefficient, see Steckler et. al.(1982) and Emmons (1988).

The work done on the flow through horizontal vents, such as the one shown in figure 1, is very limited. The flow rate can be estimated, as done for vertical vents, by using Bernoulli's equation (Emmons,1988). However, this model breaks down for problems where both density and pressure differences exist across the vent giving rise to significant buoyancy effects in addition to the pressure effect (Cooper, 1990). Some experimental work has been done on the buoyancy driven flow through horizontal vents for the special circumstance of zero pressure difference across the vent $\Delta p = 0$ (Brown, 1962, Epstein, 1988). In this case, the flow is bidirectional with the flow rates in the two directions, across the vent, being equal for a single vent due to continuity. Epstein used water/brine as the fluid and studied in detail the effect of varying the length to diameter (L/D) ratio of the horizontal vent. He identified different flow regimes and termed these as oscillatory exchange flow, Bernoulli flow, combined turbulent diffusion and Bernoulli flow, and turbulent flow.

American Society of Mechanical Engineers (ASME). National Heat Transfer Conference. Visualization of Heat Transfer Processes. HTD-Vol. 252. August 1993, Atlanta, GA, Am. Soc. of Mechanical Engineers, New York, NY, 1-17 pp, 1993.

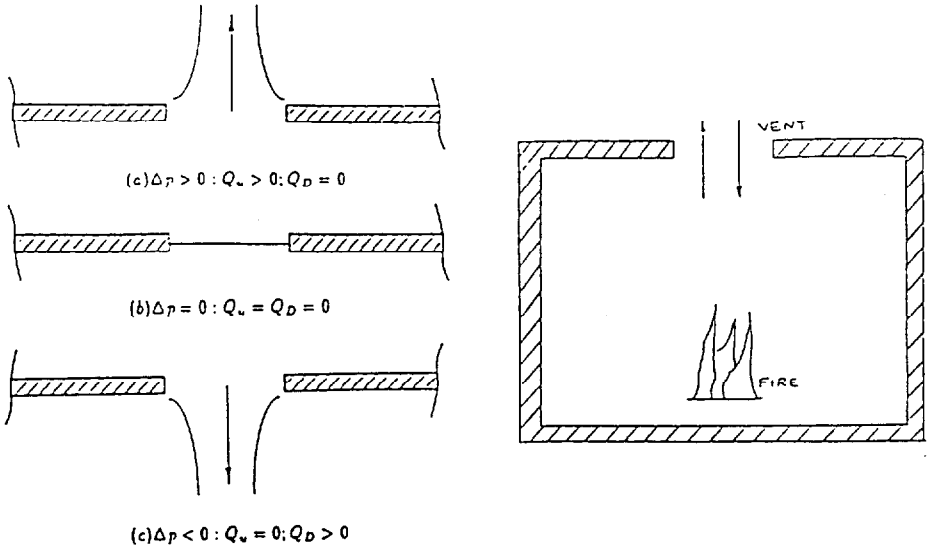

Figure 1: A typical enclosure with a horizontal vent, along with the standard vent flow model based on Bernoulli's equation.

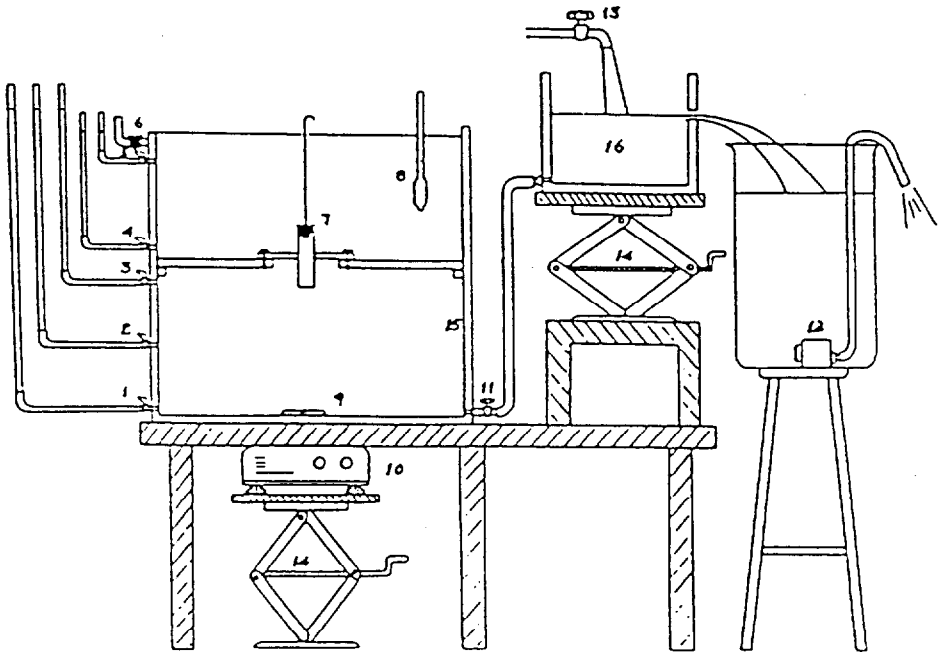

1 ~ 5: Manometers 1 ~ 5.
6: Stopper for overflow notch.
7: Stopper for vent openning.
8: Hydrometer.
9: Magnetic stirring bar
10: Magnetic Mixer.
11: Control valve
12: Suction Pump.
13: Faucet.
14: Lifting jack.
15: Plexiglass tank.
16: Storage tank.

Figure 2: Sketch of the experimental arrangement for the water/brine system.

The standard vent-flow model, based on Bernoulli's equation, assumes unidirectional flow and breaks down if a bidirectional flow exchange occurs under the combined effects of buoyancy and pressure. This model predicts zero flow when $\Delta p = 0$. This is obviously incorrect since flow arises due to the buoyancy effects, as mentioned above. With increasing pressure difference Δp, the bidirectional flow is replaced by unidirectional flow. The conditions under which this transition in the flow regime occurs is termed as purging or flooding. Thus, at purging, the pressure difference is large enough to overcome the buoyancy effects. Here, Δp is defined as

$$\Delta p = p_l - p_u \qquad (1)$$

where, p_l and p_u are the hydrostatic pressures at the vent elevation in the lower and upper environments, respectively. If $|\Delta p|$ exceeds some critical value, $|\Delta p_c|$, then the flow becomes unidirectional and the flow in the direction opposite to the exerted pressure becomes zero. Thus, the problem of flow through a horizontal vent is governed by the three variables L/D, Δp and $\Delta\rho$, where $\Delta\rho$ is defined as

$$\Delta\rho = \rho_u - \rho_l \qquad (2)$$

and the subscripts u and l refer to the upper and lower environments, respectively. The pressure acts to force the flow against the buoyancy effect in many practical situations such as enclosure fires mentioned earlier. Thus, as shown by Tan and Jaluria (1992), the transport processes across the vent may be characterized in terms of the two dimensionless variables L/D and the buoyancy parameter B, where

$$B = g\,\Delta\rho\,D / \Delta p \qquad (3)$$

A few other studies have considered the buoyancy-induced flow through openings in enclosures. The work of Takeda (1990) was largely directed at fires in ships. Experimental studies were carried out to determine the effect of the vent flow on fire growth and spread. Heskestad and Spaulding (1989) carried out an experimental study on the inflow of air to a fire space through wall and ceiling apertures needed to prevent escape of smoke. The fluid mechanics of natural ventilation has been considered experimentally and analytically by Linden et. al. (1990), to bring out the important basic characteristics of these flows. Tan and Jaluria (1992) carried out an experimental study on the flow across horizontal vents with applied pressure and density differences in a water/brine system, focusing on the resulting flow rates.

This paper presents a detailed experimental study on the visualization of the flow across a horizontal vent in an enclosed region for arbitrary values of the governing variables $\Delta\rho$, Δp and L/D. Two different experiments are carried out. In the first case, fresh and saline water are employed to simulate the density difference. Visualization is used to determine whether the flow is unidirectional or bidirectional and to study the main characteristics of the transport processes. The flow rates across the vent are also determined and considered in terms of the observed flow behavior. The second experiment deals with air as the fluid and a temperature difference across the vent is used to obtain the desired density difference. Visualization is used to determine the nature of transport across the vent, particularly its transient characteristics, and whether a bidirectional or a unidirectional flow exists under the specified conditions. Flow visualization is particularly valuable in this problem and is considered in terms of the overall transport mechanisms.

EXPERIMENTAL ARRANGEMENT

Water/Brine System

The experiments are carried out in a rectangular tank made of Plexiglas to allow flow visualization. The tank is 0.74 m long, 0.44 m wide and 0.62 m high. A metal frame support is provided on all sides and at the bottom. A horizontal Plexiglas plate is attached to a 1.0 cm wide ledge constructed all the way around inside the tank at a height of 0.31 m from the bottom. This partition separates the two fluid regions at different densities. Vents of different lengths and diameters, for a variety of L/D ratios, were fabricated. These could be attached to the partition by means of a support plate located at the opening in the partition, as shown in figure 2. The value of L/D could be varied, employing vents of very small diameters for those with L/D values of around 6.0.

The density difference $\Delta\rho$ between the fluids in the two regions is obtained by fixing the salinity level in the brine solution, varying the density difference ratio $\Delta\rho/\rho$ from 0.0 to about 0.2. The salinity is measured by means of a range of hydrometers, obtaining error of less than a few percent in the density measurements. The pressure difference Δp across the vent is obtained by keeping the upper region open to the atmosphere and pressurizing the bottom region. The pressure differences that arise in typical compartment fires are very small, with $|\Delta p/\Delta p_c|$ being around 0.2 or less (Cooper, 1990). The purging pressure difference Δp_c is of the order of $(g\Delta\rho D)$, for a vent of zero height L. This yields a value of 39.2 N/m^2 for typical values of D = 0.02m and $\Delta\rho$ = 200 kg/m^3. This is a relatively small value and is easily obtained by the simple arrangement shown in figure 2. The arrangement imparts the required pressure difference due to the gravitational head provided by a reservoir which can be moved vertically. The upper region is kept open to the atmosphere and the lower region is connected at the bottom of the tank to the reservoir, which contains fresh water. The imposed pressure difference is varied by moving the reservoir vertically. These pressure differences are measured by means of a manometer as well as a low pressure differential transducer made by Omega. Several pressure taps are located on the side of the tank and these may be attached to the manometer or the transducer to yield the pressure difference, employing appropriate taps for a given configuration. As

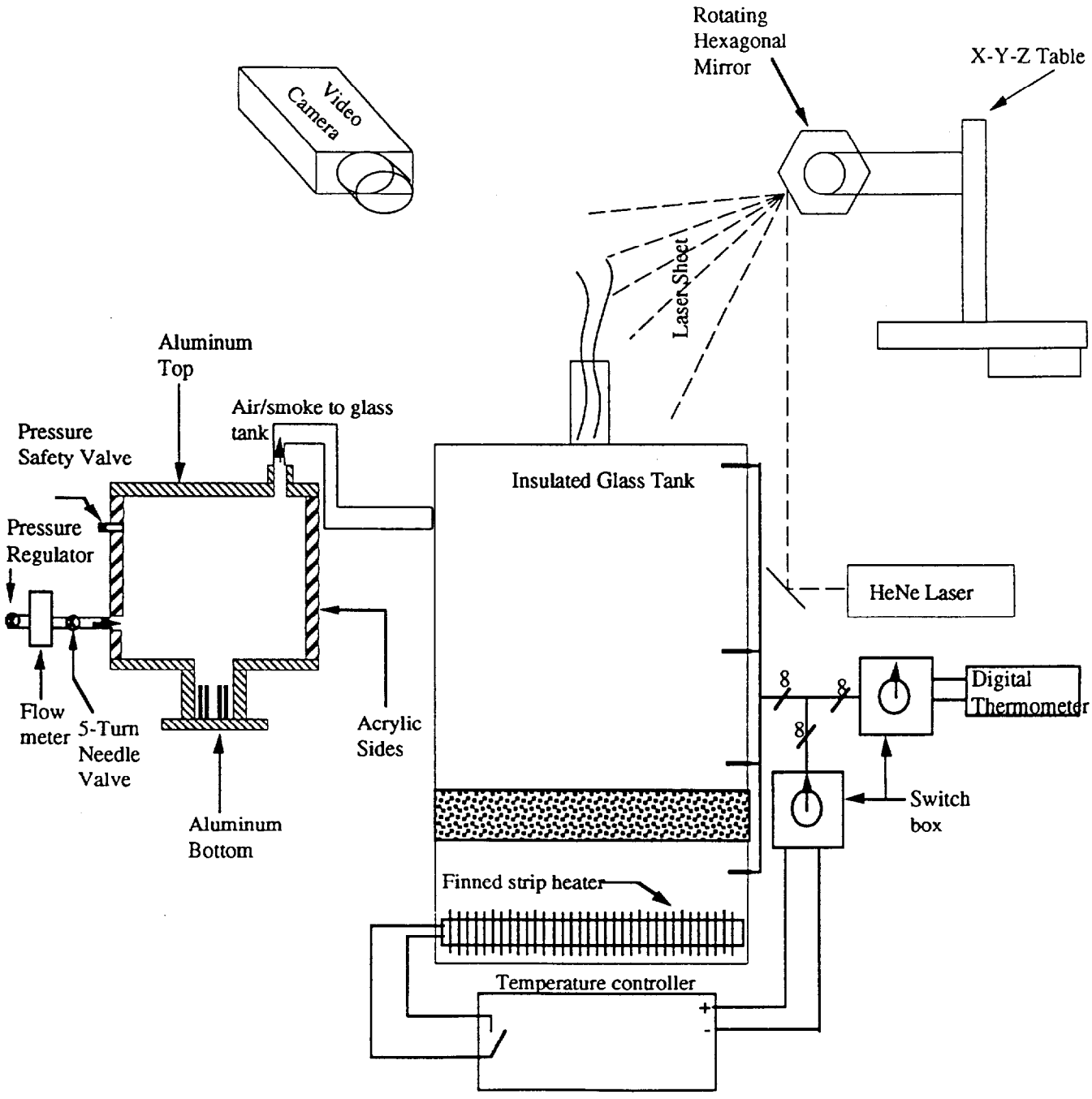

Figure 3: Schematic showing the four sub-systems of the experimental set-up for air as the fluid.

expected, the pressure variation far from the flow region is due to the hydrostatic variation.

The volume flow rate across the vent Q is obtained by measuring the dilution of the brine solution contained in the upper region, as discussed by Epstein (1988) and Tan and Jaluria (1992). If the pressure difference $\Delta p = 0$, a bidirectional flow arises across the vent, with the upflow equal to the downflow. Similarly, for $\Delta p = 0$, the net upward and the downward flow can be obtained by measuring the dilution and the inflow into the lower region, as discussed in detail by Tan and Jaluria (1992). The vent is opened for a short period of time and the flow across the vent is obtained. From this, the average flow rate over the given time period is determined.

The flow field near the vent is observed during the experiment by means of visualization. Initially, a dye was employed for visualization. However, a more convenient and non-intrusive approach is to use optical methods. Because of the fairly large density differences that arise, a shadowgraph yields the flow pattern quite clearly. A projector was placed at the back of the tank while a smoke glass screen was placed in the front. The essentially parallel light beam generated by the projector passes through the section around the vent opening. Because of the difference in optical density due to the fluid density differences, a shadow of the density variation in the test section is projected on to the screen. Thus, the phenomena of interest could be observed or photographed. The sharpness of the image on the screen depends on the size of the light source. By tracing the most deflected rays emerging from an extended light source, it can be shown that the lack of image sharpness is approximately given by ld/f, where d is the source diameter, l is the distance between the screen and the center of the test section and f is the focal length of the projector. It follows that the source should be small. The projector was placed 1.0 m away from the tank and the screen 0.05 m from it in order to obtain the clearest shadow on the screen, which was then photographed or videotaped. Thus, this visualization allows the determination of the transition from a bidirectional to a unidirectional flow as Δp is increased for a given density difference $\Delta \rho$. The flow characteristics, particularly the transient behavior, are also investigated.

Heated Air System

The experimental set-up for this case consists of four sub-systems. As shown in figure 3, these are the glass tank, the temperature measurement and regulation system, the pressure measurement and regulation system and the flow visualization system. The interior of the tank measures 0.41 m x 0.41 m x 0.46 m. The top, front, back and left side of this enclosure consisted of double-panel, 6.35 mm thick Crystal-Clear glass with a 9.53 mm air-gap, while the bottom and inlet-side consisted of 9.53 mm glass-Melamine composite (G-10). To accommodate a horizontal vent, 0.051 m diameter holes were cut concentrically into the two glass panels at the top. All the interior edges and corners were sealed with a three-layer application of silicone, high temperature Teflon adhesive tape and silicone, while all incoming wire and duct fittings were sealed with O-rings. It was confirmed that the leakage of air from the tank was negligible.

To monitor the temperature within the glass enclosure, type-T thermocouples were mounted vertically along the wall. The outputs of these thermocouples were fed into two, parallel, switch boxes. The output of one switch box is connected to a digital thermometer for temperature monitoring, while that of the second switch box was connected to an Omega CN9112 temperature controller which operated two 0.38 m, 10.5 W finned strip heaters connected in series. To achieve uniform conditions in the tank, a layer of diffusive material was added. It consisted of copper nettings sandwiched between two perforated aluminum sheets. By layering the nettings uniformly, effective flow diffusion was achieved. Also, the copper nettings added temperature stability by providing thermal capacitance.

On the top of the G-10 inlet side, a pressure tap was placed. Due to the low pressures of interest, mean flows within the enclosure rendered accurate pressure readings difficult. Therefore, a diffuser for the inlet as well as a buffer for the pressure tap were added, as shown in figure 4. A low-pressure transducer (Omega PX653-0.1D5V) with a range of 0-2.5 mm of water and an accuracy of 0.5% was employed for the pressure measurements. A stagnation chamber was used to pressurize the glass enclosure. This chamber had an inside dimension of 0.15 m x 0.15 m x 0.15 m. Its pressure was raised by a compressor, and controlled by a Fairchild model 10 pneumatic pressure regulator and a 5-turn needle valve. A Rotameter type flow meter was connected upstream of this chamber to measure the mean flow rate.

Smoke was introduced into the stagnation chamber by burning incense or by evaporating kerosene. To increase temperature uniformity and to minimize the buoyancy effect of the smoke, the top and bottom of the stagnation chamber were constructed out of 12.7 mm thick aluminum plates. During the experiment, the temperature of the smoke inside the glass enclosure was measured to be no more than 0.5 ^{o}C above ambient. The pressurized air/smoke from the stagnation chamber was fed into the glass enclosure via a diffuser, as shown in figure 4. As mentioned earlier, the purpose of the diffuser was to prevent the entering air/smoke from introducing large-scale recirculating motion in the tank. Also, the diffuser was fitted with a slight vertical grade to prevent any oil accumulation which could cause pressure fluctuations.

To visualize the flow in the duct, a vertical laser sheet was passed through the center of the exit duct, and the resulting scattering off the smoke particles were recorded. The laser sheet was created by reflecting the output of a 632.8 nm, 35mW HeNe laser beam off a hexagonal mirror-assembly rotating at 2000 RPM. This corresponded to a frequency of 12 kHz. The mirror assembly consisted of a high-strength tool-steel hexagonal cylinder. The weight of tool-steel provided rotational inertia, while its hardness provided dimensional stability. One end of this cylinder was machined to press into a high-speed ball-bearing, while the other end was machined concentric to the first with a blind hole at the center to accommodate the shaft of a DC motor (TRW 403A159). Since first-face mirrors are clipped onto

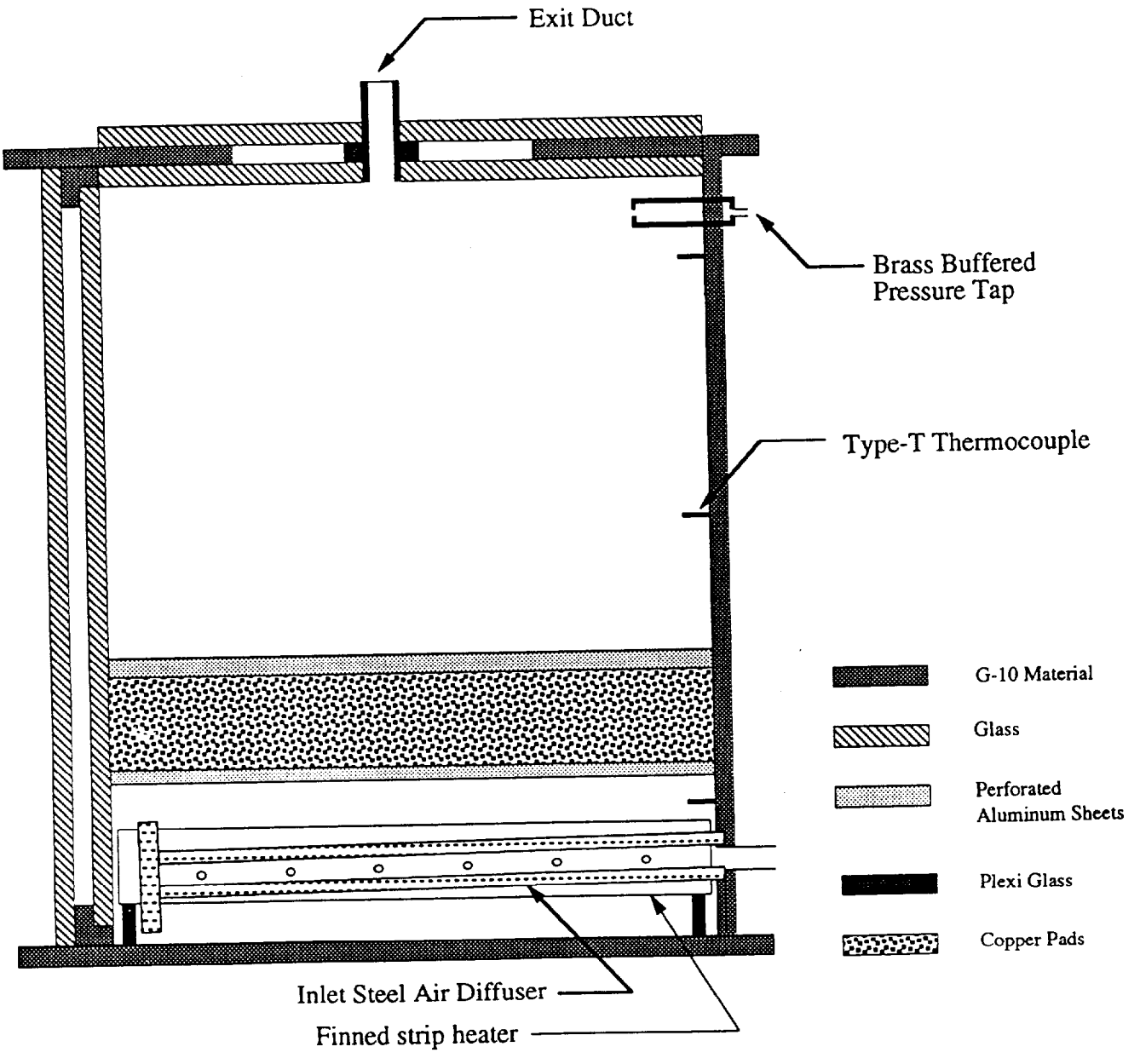

Figure 4: Schematic showing the components of the glass tank for air as the fluid.

each of the six faces of the hexagonal cylinder, they must be co-planar to the axis of rotation to very tight tolerance, otherwise the sheet would vibrate and thicken. The faces of the present hexagonal cylinders were co-planar to the axis of rotation to better than 0.0127 mm. The rotating hexagonal mirror assembly was mounted on top of an XYZ traversing rack. The laser beam was passed along all the axis of motion in such a way that visualization at any location could be performed without realigning the laser beam.

In performing the experiment, sufficient time was allowed for the entire system to reach steady state. Once steady state was achieved, the internal temperatures were measured before and after the experiments to ensure uniform temperature. Typically the measurements showed a temperature difference between the top and bottom of the glass tank to be less than 5 % of the average value. Most importantly, the top region near the exit duct attained temperature uniformity of better than 1 %. Also the ambient temperature and pressures were recorded before and after each experiment.

EXPERIMENTAL RESULTS

Water Flow System

Several interesting and important results have been obtained. Using the shadowgraph for flow visualization in the water/brine system of figure 2, a bidirectional flow was found to arise across the vent at $\Delta p = 0$, with denser fluid descending in the central portion of the opening and lighter fluid rising in the outer portion. Figure 5 shows the resulting bidirectional flow for two different density differences $\Delta\rho$. Even though the appearance of the flow is similar to that of a turbulent jet, the velocities are very low, being of order 1 cm/s, and the flows are laminar since the Reynolds number based on the vent diameter is of order 100. The mass diffusivity of salt in water D_{AB} is very small, being around 1.2×10^{-9} m^2/s. This gives a Lewis number $Le=\alpha/D_{AB}$, where α is the thermal diffusivity of water, of around 120. Therefore, the salt diffuses out very slowly, giving the impression of a turbulent jet.

As mentioned earlier, the volume flow rates were found to be the same in the two directions due to continuity. This flow rate Q was measured by Tan and Jaluria (1992). A smaller density difference was found to give rise to a smaller flow rate Q across the vent. A comparison with earlier work on this circumstance indicated good agreement. The dependence of Q on L/D follows the trend predicted by Epstein (1988), lending support to these measurements.

As the opposing pressure difference Δp is increased, this downward flow is found to decrease, ultimately giving rise to a unidirectional upward flow. This purging, or flooding, pressure difference Δp_c is of order of $(g\ \Delta\rho\ L)$ for a vent of height L. Therefore, for typical values of L = 0.1 m and $\Delta\rho = 100$ kg/m^3, $\Delta p_c = 98$ N/m^2. As mentioned earlier, a differential pressure transducer of around 250 N/m^2 full scale was used for these pressure measurements. Figure 6 shows the shadowgraph pictures of the flow close to purging conditions for two different values of the pressure difference Δp. Clearly, only the flow into the upper region is observed in (b), with only a small downward flow in (a). However, the flows were observed to be quite steady with very little transient variation. As will be seen later, \this aspect was found to be very different with air.

Figure 7 shows the flow pattern as Δp is decreased at a given value of the density difference $\Delta\rho$. Thus, the flow is unidirectional in (a) and becomes bidirectional, with the downward flow increasing as the pressure difference Δp is decreased. Finally, the pressure in the lower region becomes much less than that in the upper region, resulting in a unidirectional downward flow in (d). Thus, the flow is unidirectional in (a) and (d), with pressure effects dominating over the buoyancy effects and the flow changing direction depending on the sign of Δp. Both the pressure and buoyancy effects are significant in (b) and (c), with the buoyancy parameter B of order unity, giving rise to flow into both the regions.

Figure 8 shows some typical results on the flow rates obtained for nonzero Δp and $\Delta\rho$, considering a vent of negligible height (L/D = 0). The results are shown in terms of the experimental data and the corresponding correlating equations for the net flow Q_O and the upward flow Q_U. It is clearly seen that the two flow rates increase with increasing Δp and decrease as the density difference is increased, as expected from the physical mechanisms discussed above. There is some scatter in the data. This is largely due to the difficulty of maintaining the small pressure differences of interest and the errors in measuring the small flow rates that arise. Also, these results are obtained by varying $\Delta\rho$ and Δp over wide ranges of interest. The flow itself was found to be quite steady, with no significant fluctuations.

Some typical results on the variation of the flooding pressure difference Δp_c with $\Delta\rho$ at a given value of L/D are shown in figure 9. The measured values are in the range that may be derived on the basis of scale analysis. The results were found to be repeatable, within a few percent of the measured values. However, the transition from bidirectional to unidirectional flow was found to be a fairly gradual one, indicating the downflow Q_D to gradually reduce to zero as the pressure difference Δp is increased. With increasing values of $(g\ \Delta\rho\ D)$, at a given L/D, the purging pressure difference Δp_c was found to increase, as expected. Several other similar results were obtained and figures 8 and 9 show the typical observed trends. Results were obtained for a wide range of L/D ratios. The trends were found to be quite sensitive to the value of L/D. At very low pressure differences, the buoyancy effects dominate the flow across the vent, giving rise to a bidirectional flow. Thus, clearly the basic trends indicated by Cooper (1990) are obtained. Additional results on the flow rates for this circumstance were obtained by Tan and Jaluria (1992).

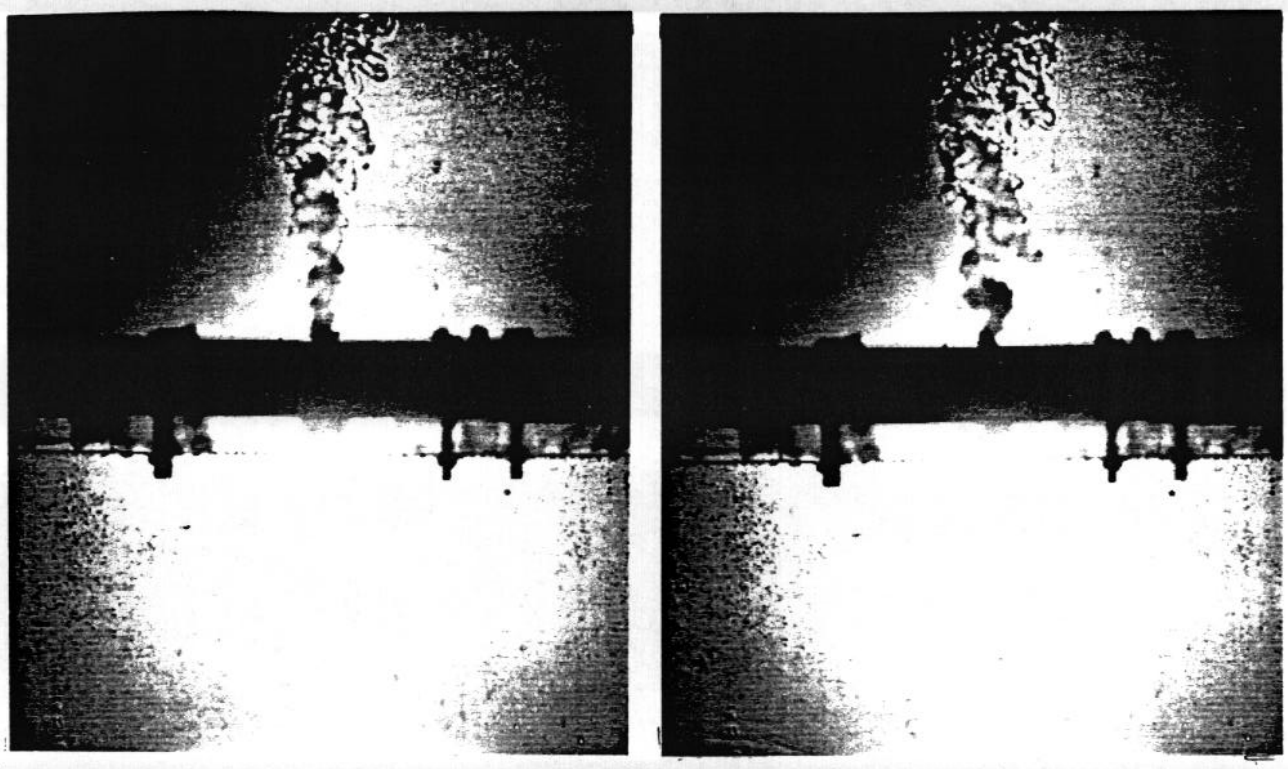

a) b)

Figure 5: Shadowgraph pictures for the experiments with $\Delta\rho = 0$ and L/D = 1.0 in water. (a) D = 0.0445 m, $\Delta\rho$ = 39.6 kg/m^3 ; (b) D = 0.0254 m, $\Delta\rho$ = 84.2 kg/m^3.

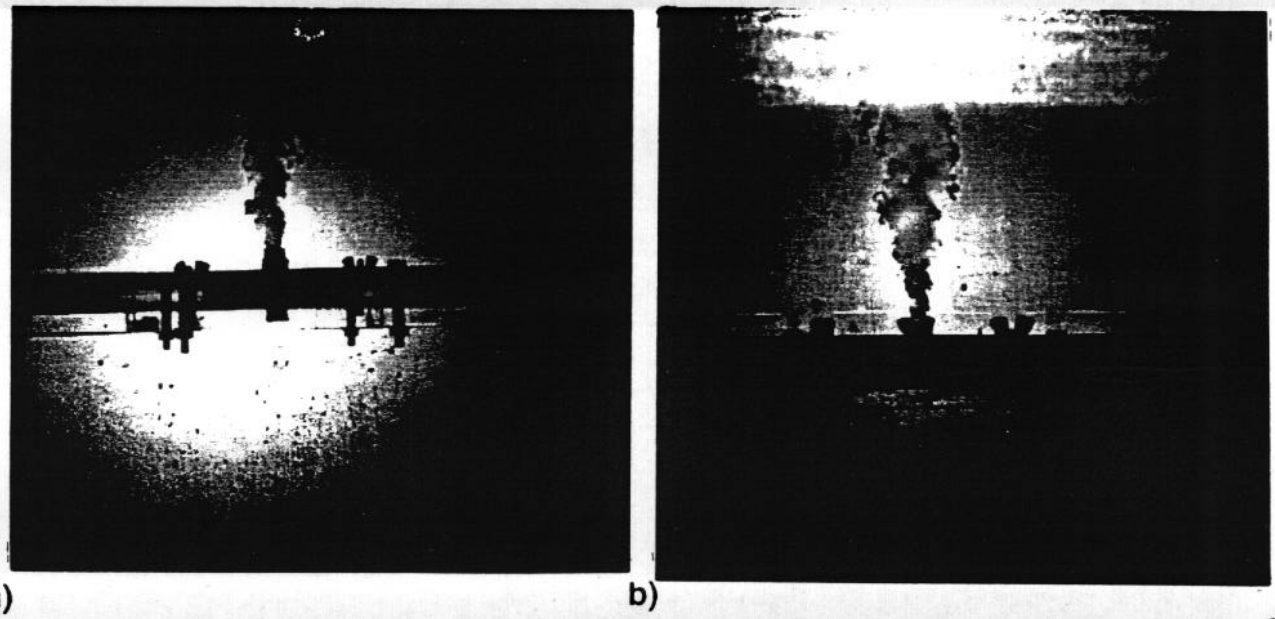

a) b)

Figure 6: Shadowgraph pictures of the flow close to purging conditions in water at L/D = 2.75 and $\Delta\rho$ = 62.5 kg/ m^3. (a) Δp = 14.92 N/m^2 ; (b) Δp = 22.7 N/m^2 .

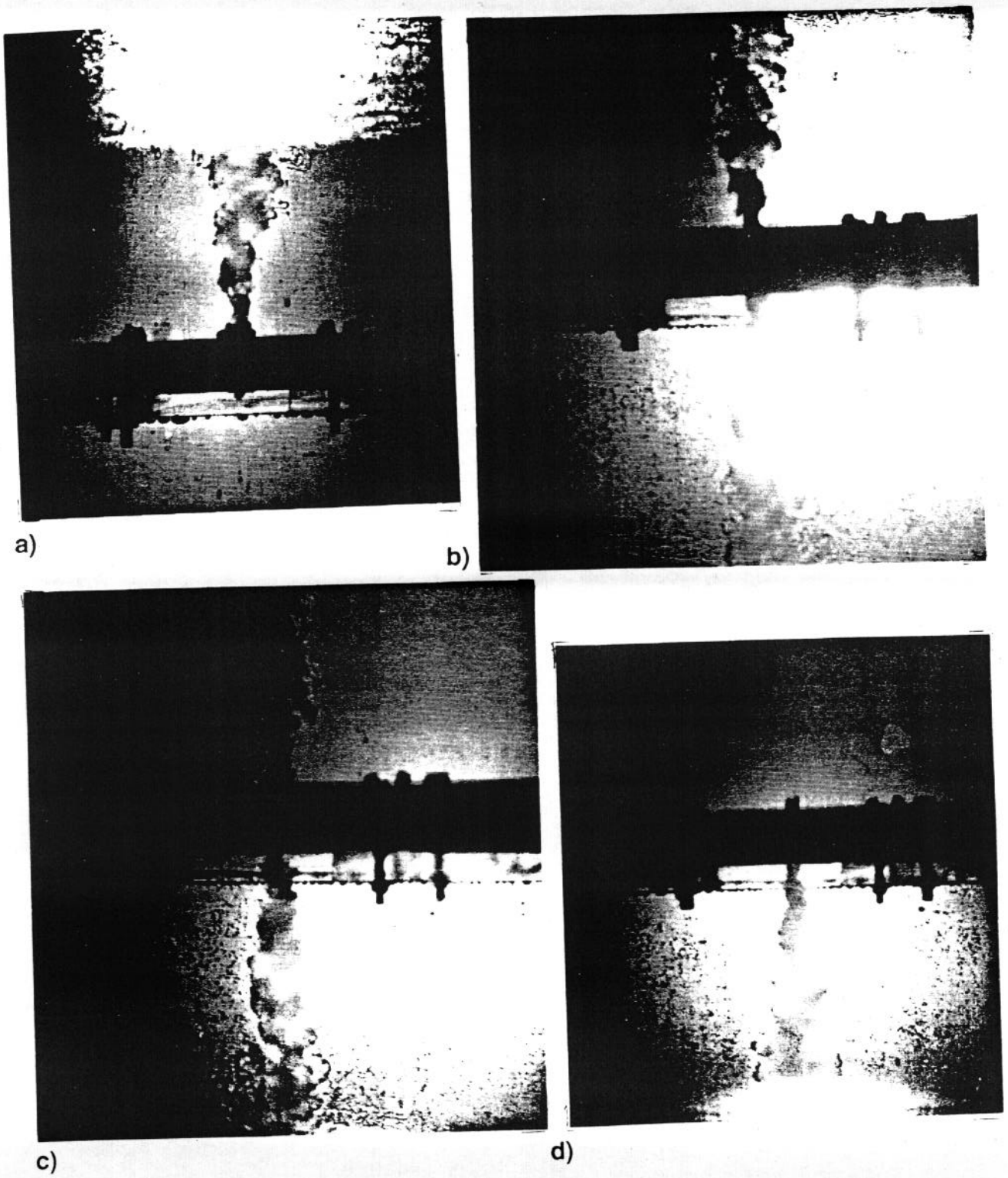

Figure 7: Effect of decreasing pressure difference Δp at a given value of $\Delta \rho$ for a vent in water.

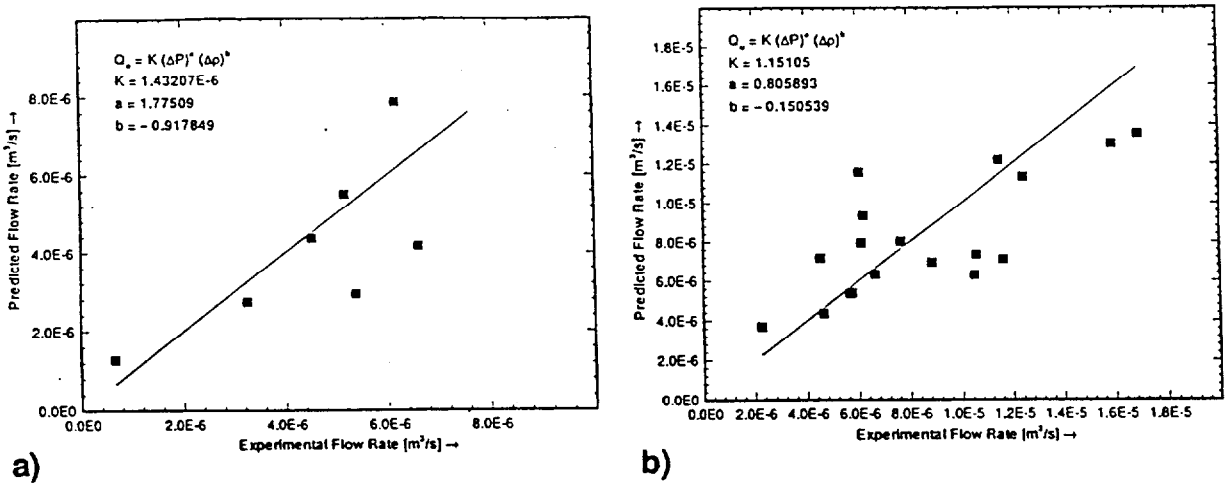

Figure 8: Comparison between experimental data for water and the predicted values from the correlating equations for the net flow rate Q_O and the upward flow rate Q_U.

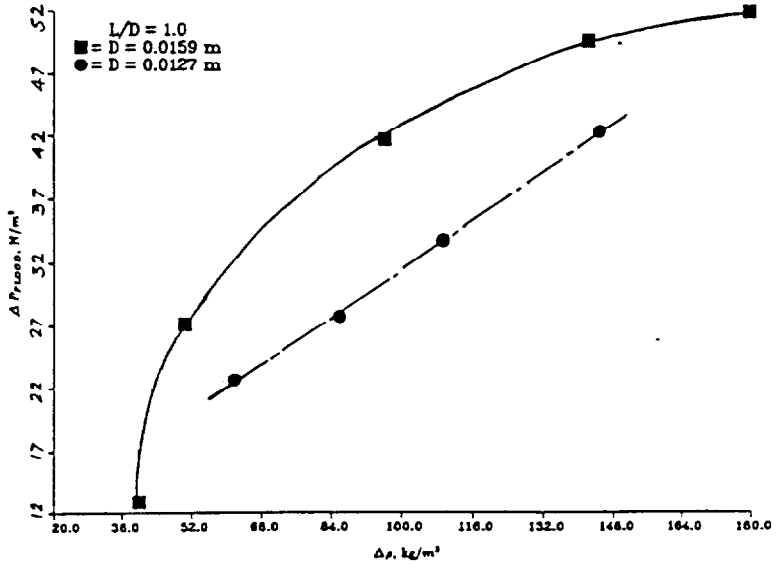

Figure 9: Purging pressure as a function of the density difference at L/D = 1.0 for the water/brine flow.

Air Flow System

The air flow arrangement has been discussed in detail in the preceding section. The main difference is in the fluid, largely in the essentially incompressible nature of water as compared to air. As a consequence, we may expect interesting differences in the transient behavior of the flows generated across the vent. Employing the smoke laser sheet arrangement described earlier, the flow pattern could be visualized to study the basic characteristics of the flow resulting from the imposed pressure and temperature differences across the vent. Again, vents of various L/D ratios were considered.

Figure 10 shows some of the possible modes of flow across a vent with an L/D ratio of 1.0, B=5.54 and nonzero pressure and temperature differences. Four of these modes were previously found by Epstein (1988), and can be described as: Inflow at the left and outflow at the right (figure 10a), outflow at the left and inflow at the right (figure 10b), outflow at the center (figure 10c) and inflow at the center (figure 10d). These modes were transient in nature and were found to vary from one to another with time. In fact, figure 10e shows a frame in which the modes of motion have rotated out of the plane of visualization. Interestingly, one mode of motion that was not previously found was that of a unidirectional flow (figure 10f). Apparently, even though the net flow, averaged over time, is upward, the transient effects are sufficiently large to make the flow reverse direction with time. A similar behavior was found for a smaller diameter duct with an L/D ratio of 4.0 and B of 0.1 (figure 11b-e), in which a unidirectional flow would have arisen for this value of B in the water/brine system. Figure 11a shows the flow when no temperature difference is present. Thus, this is a pressure driven flow, with no opposing buoyancy effects. This flow is found to be quite steady, without the reverse flow situations seen for significant buoyancy cases.

The flow pattern was also found to exhibit many different variations, depending on the value of the buoyancy parameter B and the L/D ratio. Some of these patterns are shown in figure 12. Clearly, different flow regimes arise and the flow is much more complex than that observed for water. The net flow rates may be measured, but the flow across the vent is a time-dependent phenomenon unless the pressure difference is very high or the buoyancy effect is very small, indicated by a very small value of B. In many cases, recirculating flow was found to arise with upward flow on one side of the vent and downward flow on the other side, even for relatively high pressure differences. Since the time-dependent flow across the vent is important in the modeling of a fire in a vented room or compartment, it is important to study the net flow rates across the vent as well as the transient effects. The present results indicate the complexity of the problem and the need for a more detailed study of the transient effects in the transport.

Figure 13 indicates some measure of this oscillatory flow behavior for different vent geometries. The flow was videotaped and the results were analyzed for the inflow and outflow (from the lower region to the upper region) characteristics. Figure 13 (a) shows the time between inflows for a range of net upward mass flow rate. The net flow increases with Δp and, therefore, this may be considered as the variation with pressure. Thus, even though the net upward flow rate is positive, there is a fair amount of reverse flow and this reversal occurs periodically with a frequency that can be derived from these data. The elapsed time between periods of reverse flow as well as the duration of flow reversal decreased as the pressure difference was increased. This implies that the frequency of oscillation increases while the resulting inflow decreases as Δp increases for a given ΔT. The typical frequencies seen here are in the same range as those observed in earlier studies on fires in vented compartments (Takeda, 1990; Steward, et al., 1989). Figure 13 (b) shows the corresponding fraction of the net outflow across the vent that occurs as inflow, plotted against the net flow. Clearly, a substantial amount of inflow arises even though the net flow is outward. With increasing pressure difference, the net flow increases and the inflow decreases as expected, till finally there is no inflow at all. This is treated as the purging circumstance for this circumstance. The L/D ratio is also seen to be an important parameter, though the basic trends are the same in all cases.

The purging, or flooding, pressure for a very thin vent, L/D = 0.144, is shown in figure 14. As expected, the flooding pressure increases as the temperature-induced density difference $\Delta\rho$ increases. Also, these pressure differences are very small and are of the same order as the buoyancy effect, given by $g\Delta\rho D$. Figure 15 shows some typical results on the measured net mass flow rate across the vent as a function of the pressure difference for two values of the temperature difference. The flow rate is seen to increase with an increase in the pressure difference and to decrease with an increase in the temperature difference. Therefore, the trends are similar to those observed in water. However, the scatter in the data is much more for air than for water. This is partly due to the small pressure differences of interest, which are difficult to regulate and measure. In addition, the large transient behavior of the flow (figure 11) also contributes to this scatter.

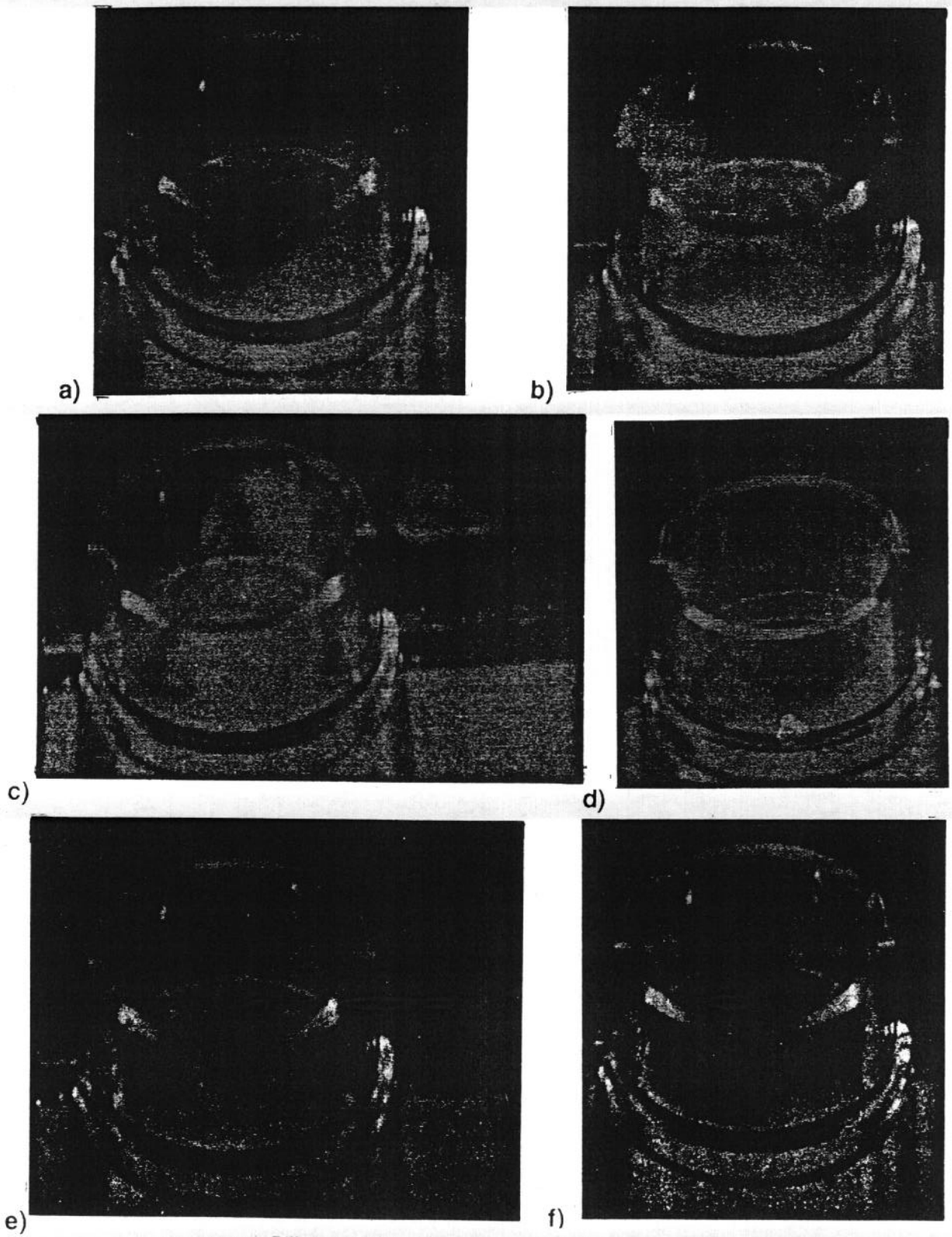

Figure 10: Different modes of flow observed for air in a vent of L/D = 1.0 and B = 5.54.

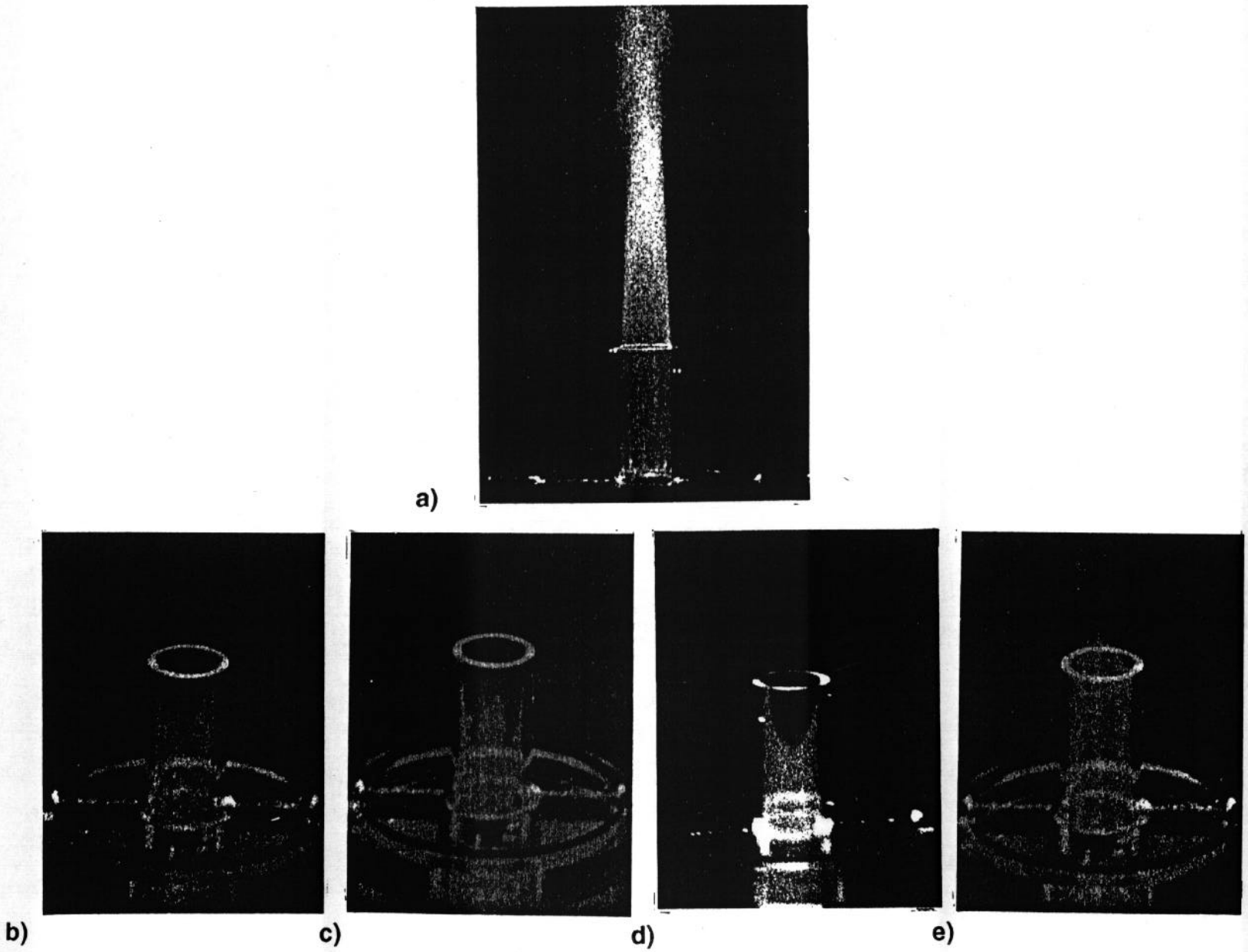

Figure 11: Flow of air in a vent of L/D=4.0 and B=0.1 with (a) $\Delta T=0$ and (b)-(e) non-zero ΔT.

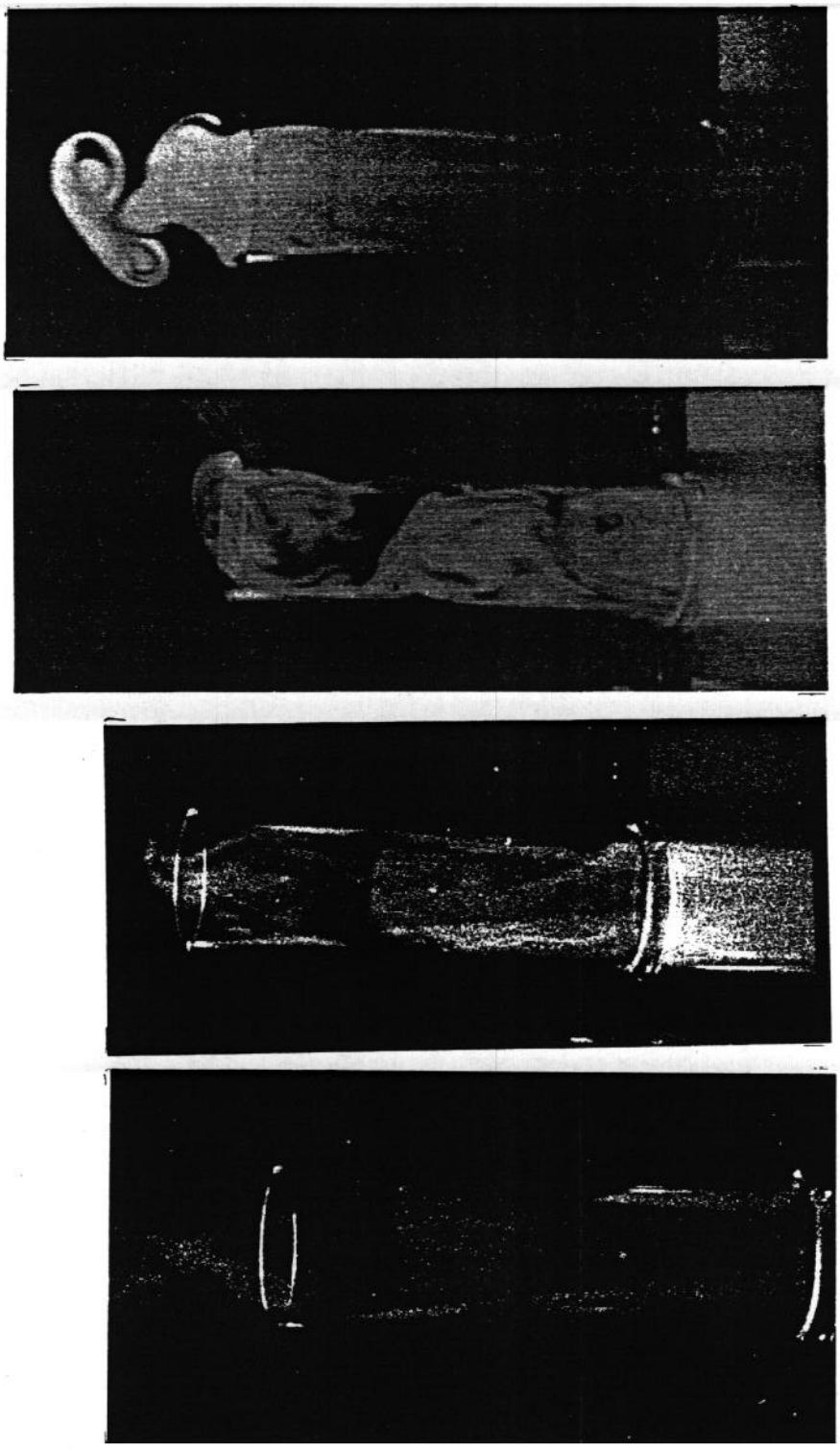

Figure 12: Different flow patterns and regimes observed for the vent flow in air.

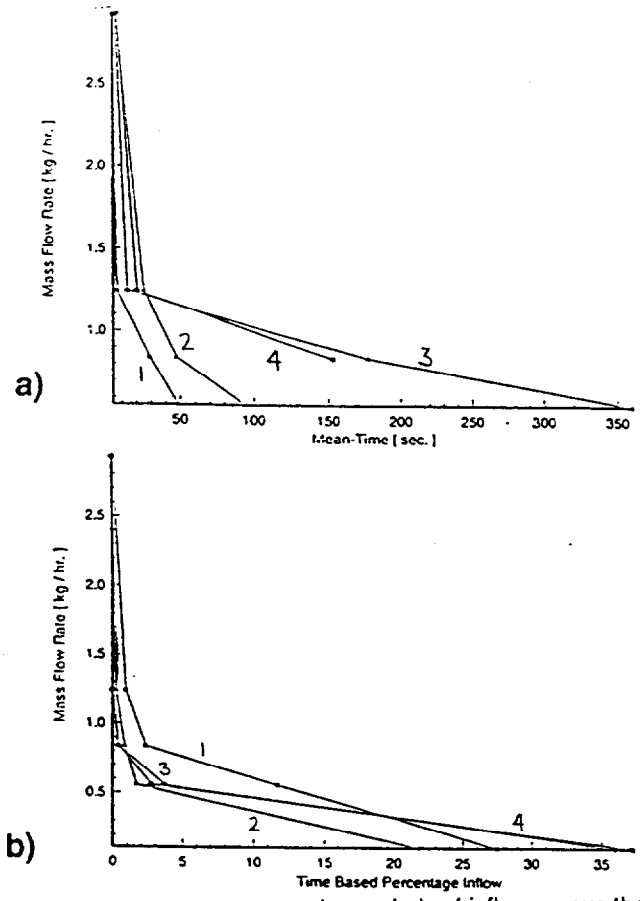

Figure 13: (a) Elapsed mean time between successive periods of inflow versus the net flow rate in air; (b) Inflow rate, as a percentage of the net flow, versus the net flow rate.
1: L/D=0.0144 2: L/D=1.0 3: L/D=2.0 4: L/D=4.0.

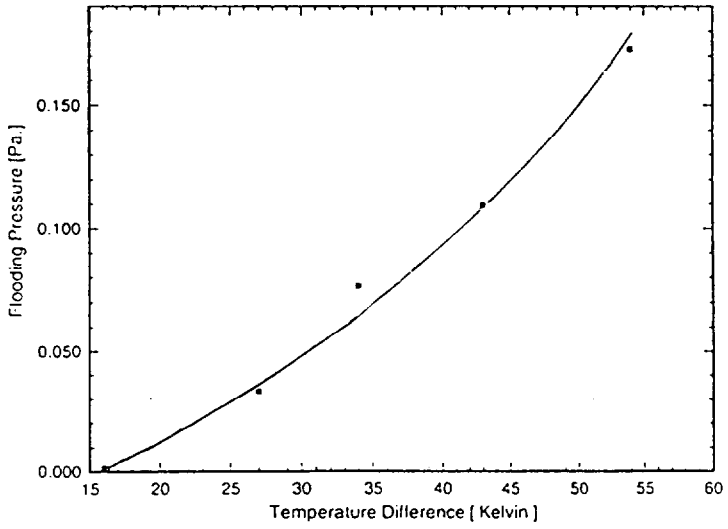

Figure 14: Variation of the flooding or purging pressure difference with the temperature difference for air in a vent of L/D=0.0144.

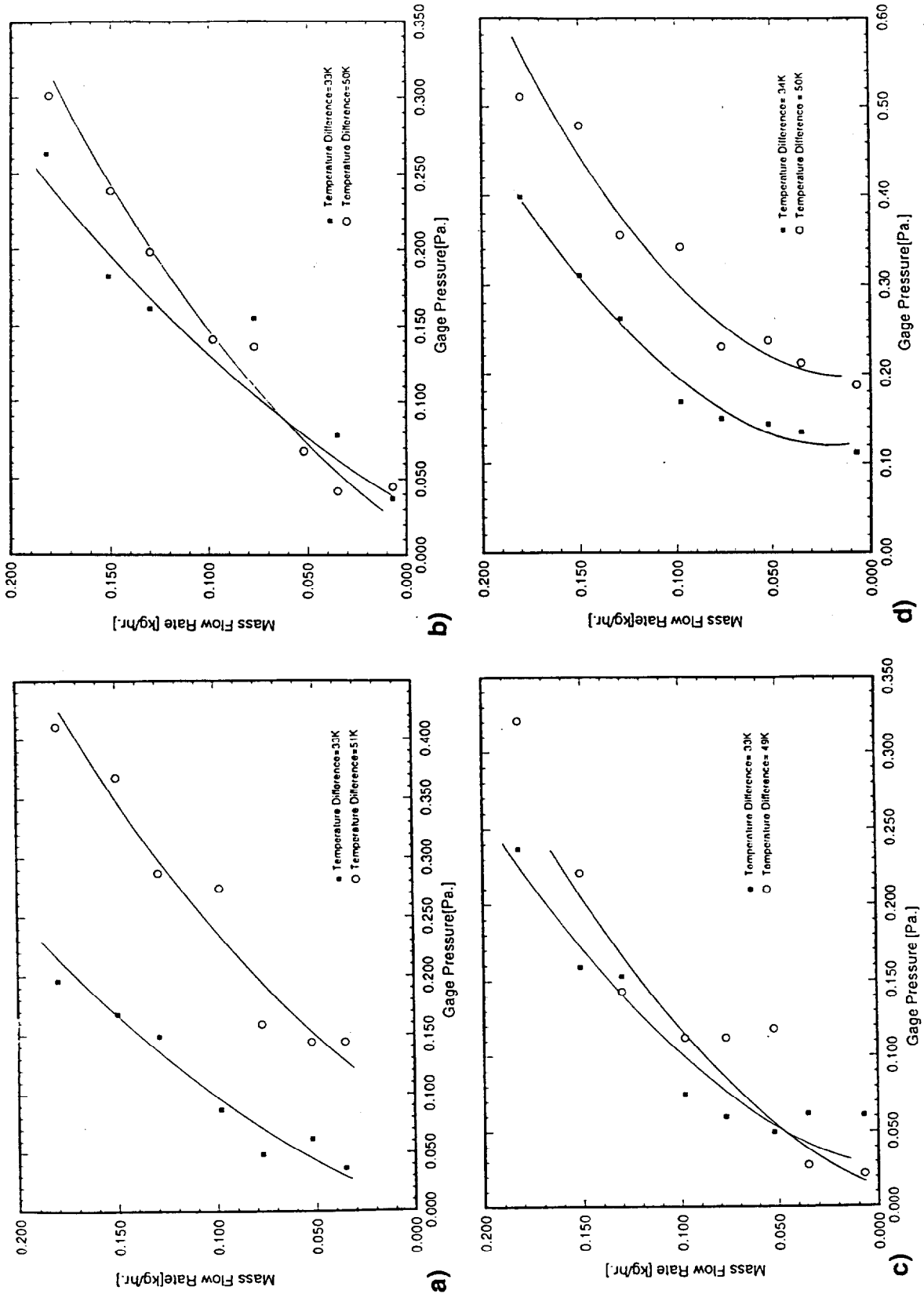

Figure 15: Variation of the net mass flow rate with the pressure difference at ΔT =37 and 55 K for air in vents of a) L/D=0.0144, b) L/D=1.0, c) L/D=2.0 and d) L/D=4.0.

CONCLUSIONS

This paper presents a detailed flow visualization study on the transport across a horizontal vent in a compartment, with nonzero pressure and density differences across the vent. This flow circumstance is of particular interest in the modeling of fires in vented compartments and in the prediction of transport in partially open enclosures. Two different flow systems, based on water/brine and air/heated air arrangements, are considered to provide the density differences over typical ranges of interest. Flow visualization is used to study the flow characteristics, particularly the transient effects and whether the flow is unidirectional or bidirectional. Though the basic trends in terms of average flow rates, purging pressure and transition from bidirectional to unidirectional flow as the pressure difference increases are similar in the two cases, strong differences are indicated by flow visualization in the transient effects that arise and in the resulting flow patterns. Transient effects are shown to be very important for the air system and the oscillatory nature of the transport processes is brought out. Flow visualization is also used to determine the flow regime and to guide the measurements of the resulting flow rates across the vent. It is seen that visualization of the flow is crucial in this important and interesting transport process. The paper also presents the differences in the visualization techniques and the nature of the transport in the two fluids.

ACKNOWLEDGEMENTS

The authors acknowledge the financial support provided by the National Institute of Standards and Technology, under Grant No. 60NANB1H1171, for this work and the several discussions with Dr. Leonard Y. Cooper on this problem. The help from Michael Phipps, Wilson Chiu and Johny I. Chowdhury in some of the experiments are also acknowledged.

REFERENCES

Abib, A.H. and Jaluria, H., 1988,"Numerical Simulation of the Buoyancy-Induced Flow in a Partially Open Enclosure," *Num. Heat Transfer*, Vol.14, pp.235-254 .

Brown, W.G., 1962,"Natural Convection Through Rectangular Openings in Partitions - 2. Horizontal Partitions," *Int. J. Heat Mass Transfer*, Vol.5, pp.869-878 .

Cooper, L.Y., 1990,"Calculation of the Flow Through a Horizontal Ceiling/Floor Vent," NIST Tech. Report, Rep. No. NISTIR-89-4052 (1989). Also, *Ann. Conf. Fire Res.*, Gaithersburg, MD (1990).

Emmons, H., 1988,"Vent Flows," *SFPE Handbook of Fire Protection Eng'g.*, Soc. Fire Protection Eng'g., Boston, Sec. 1, Ch.8.

Epstein, M., 1988,"Buoyancy-Driven Exchange Flow Through Small Openings in Horizontal Partitions," *J. Heat Transfer*, Vol.110, pp.885-893 .

Gebhart, B., Jaluria, Y., Mahajan, R.L. and Sammakia, B., 1988, *Buoyancy Induced Flows and Transport*, Hemisphere Pub. Corp., NY.

Heskestad, G. and Spaulding, R.D., 1989,"Inflow of Air Required at Wall and Ceiling Apertures to Prevent Escape of Fire Smoke," Tech. Rep., Factory Mutual Res., Norwood, MA.

Jaluria, Y., 1980, *Natural Convection Heat and Mass Transfer*, Pergamon Press, Oxford, U.K.

Jaluria,Y. and Cooper, L.Y., 1989,"Negatively Buoyant Wall Flows Generated in Enclosure Fires," *Prog. Energy Combust. Sci.*, Vol.15, pp.159-182 .

Linden, P.F., Lane-Serff, G.F. and Smeed, D.A., 1990,"Emptying Filling Boxes: The Fluid Mechanics of Natural Ventilation," *J. Fluid Mech.*, Vol.212, pp.309-335.

Quintiere, J.G., 1977, "Growth of Fire in Building Compartments," *Fire Standards & Safety*, ASTM STP,Vol.614, pp.131-167.

Steckler, K.D., Quintiere, J.G. and Rinkinen, W.J., 1982,"Flow Induced by Fire in a Compartment," 19th Symp. (Int.) Combust., Combust. Inst., Pittsburgh, PA, pp.913-920.

Steward, F.R., Morrison, L. and Mehaffey, J., 1989,"Full Scale Fire Tests for Ship Accommodation Quarters," Tech. Rep., Dept. of National Defense, Canada.

Takeda, H., 1990,"Model Experiments of Ship Fire," *22nd Int. Symp. Combust.*, pp.1311-1317.

Tan, Q. and Jaluria, Y., 1992, "Flow Through a Horizontal Vent in an Enclosure Fire," ASME Heat Transfer Div. HTD-Vol. 199, pp. 115-122.